Electronic Supplementary Material (ESI) for Lab on a Chip.

Multi-step processing of single cells using semi-permeable capsules

Greta Leonaviciene, Karolis Leonavicius, Rolandas Meskys, and Linas Mazutis

Supplementary Information

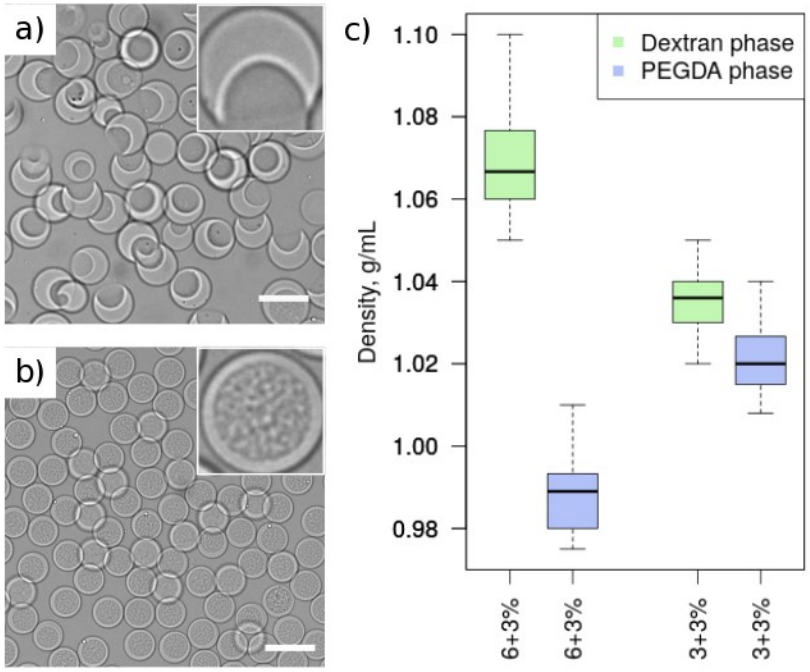

Supplementary Figure S1. Matching the density of dextran/PEGDA phases is important to achieve capsule's concentricity. *(a) Hydrogel capsules prepared using the blend composition of 6% (w/v) PEGDA (MW 8K) and 3% (v/v) PEGDA (MW 575), while in (b) 3% (w/v) PEGDA (MW 8K) and 3% (v/v) PEGDA (MW 575) was used. (c) Boxplot graph shows the density of PEGDA (shell) and dextran (core) phases after mixing the dextran/PEGDA blends and phase separation by centrifugation, as described in Material and Methods. Y-axis indicates the density and X-axis indicates the percentage of high (MW 8K) and low (MW 575) molecular weight PEGDAs. The density of the dextran phase is changing because a small fraction of PEGDA polymer mixes with dextran and vice versa. Boxplots are derived from 25 measurements of each sample. Scale bars, 50 µm.*

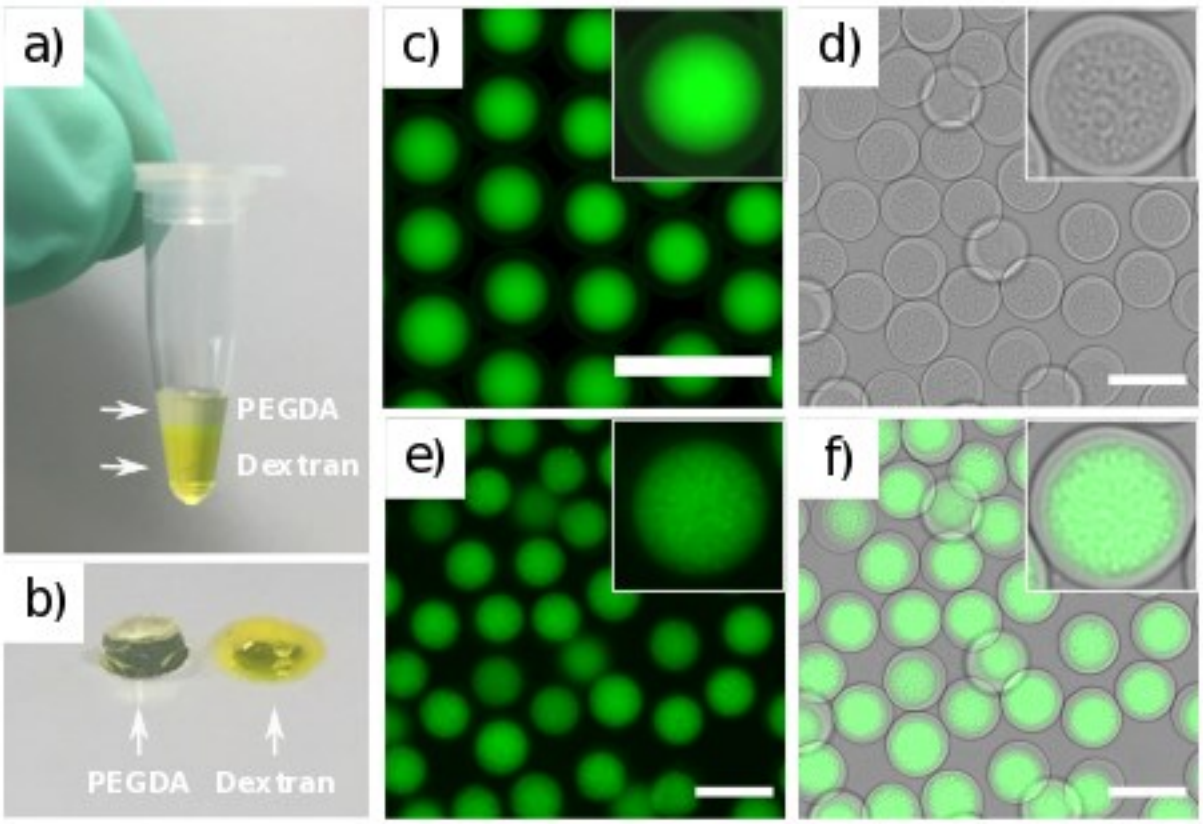

Supplementary Figure S2. Generation of concentric capsules. *Panel (a) shows PEGDA and dextran phase separation after centrifugation, where dextran phase was stained with 0.1% (w/v) fluorescein isothiocyanate-dextran (MW 500K). (b) Separation of two phases after photo-polymerization, where the PEGDA-rich phase formed hardened hydrogel, and the dextran-rich phase became more viscous and formed weak and easily breakable hydrogel. (c) Fluorescence micrograph of ATPS droplets showing the dextran phase partitioning into the core. Digital capsule micrographs of bright field (d), fluorescent (e), and merged microscopy images, respectively. Scale bars, 50 μm.*

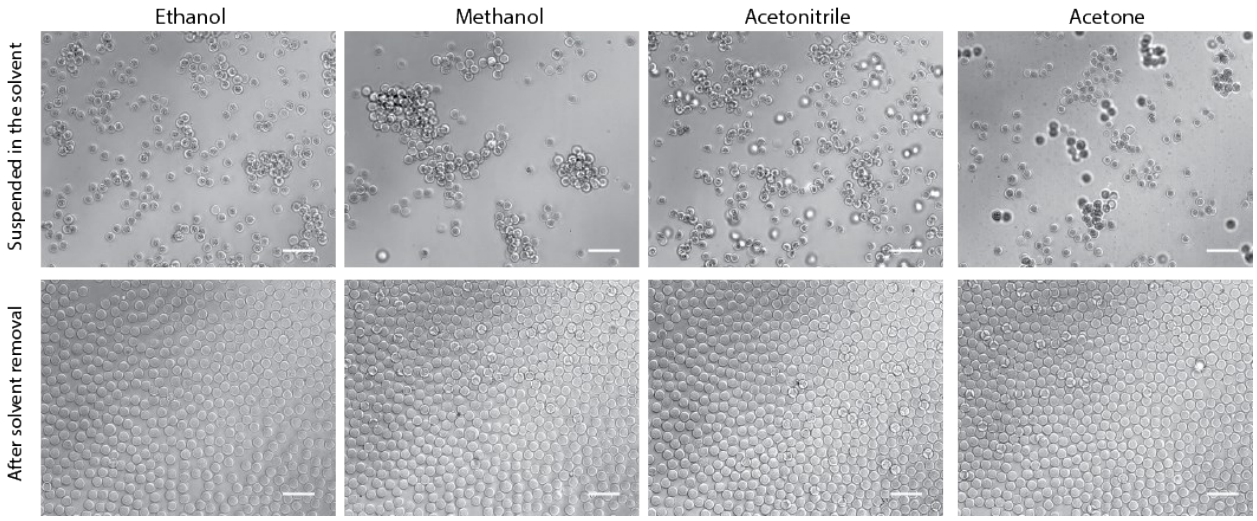

Supplementary Figure S3. **Capsules remain stable in different chemical solvents.** *20 µl of closely packed hydrogel-capsules suspended in 10mM Tris-HCl, pH [7.5] buffer were combined with 500µL of solvent; (1) 96% ethanol (AB Vilniaus Degtine), (2) 99.8% methanol (Sigma-Aldrich, 322415), (3) 99.8% acetonitrile (Sigma-Aldrich, 271004) and (4) ≥99.5% acetone (Sigma-Aldrich, 179124), and incubated at 22 ºC for 60 min. Next, capsules were centrifuged at 2000g for 5 min and washed three times with a washing buffer (10mM Tris-HCl pH [7.5], 0.05% (v/v) Triton X-100). Capsules were analyzed under the bright field microscope. Scale bars, 100 µm.*

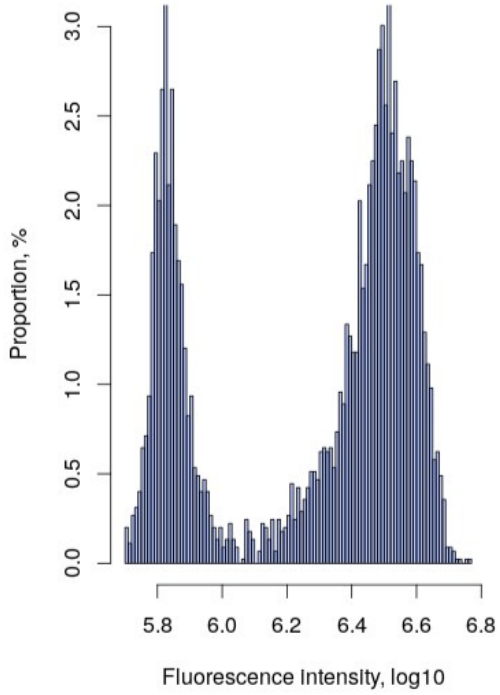

Supplementary Figure S4. **Flow cytometry analysis of capsules after single-genome amplification reaction.** *The histogram shows the fluorescence intensity distribution of 150.000 capsules, where the intensity below 6.0 represents negative and above 6.0 positive capsules, respectively.*

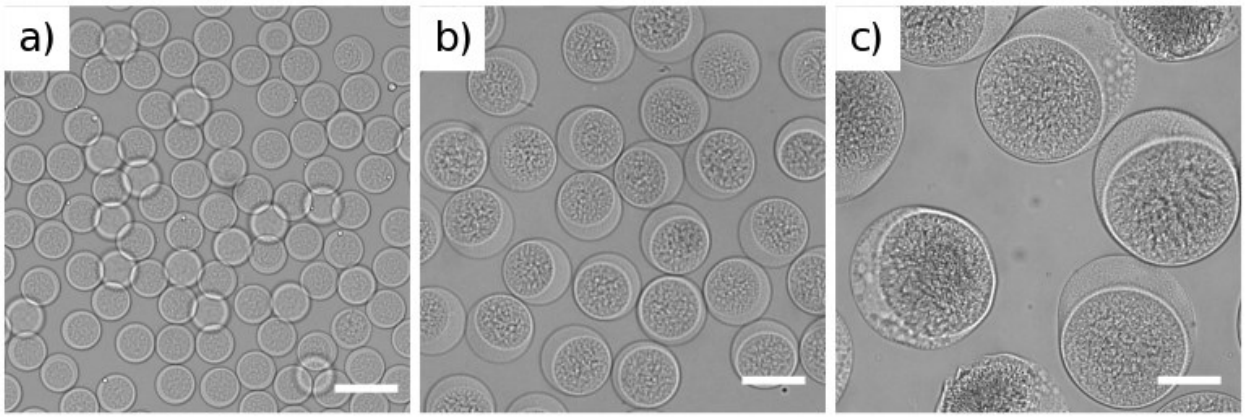

Supplementary Figure S5. Evaluation of concentricity of different size capsules. *Bright field images showing capsules of 30 µm (a), 60 µm (b) or 100 µm (c) in diameter. In all cases capsules were prepared by mixing 3% (w/v) PEGDA (MW 8K), 3% (v/v) PEGDA (MW 575) and 5.5% (w/v) dextran (MW 500K), centrifugation and co-flow emulsification. Scale bars, 50 µm.*

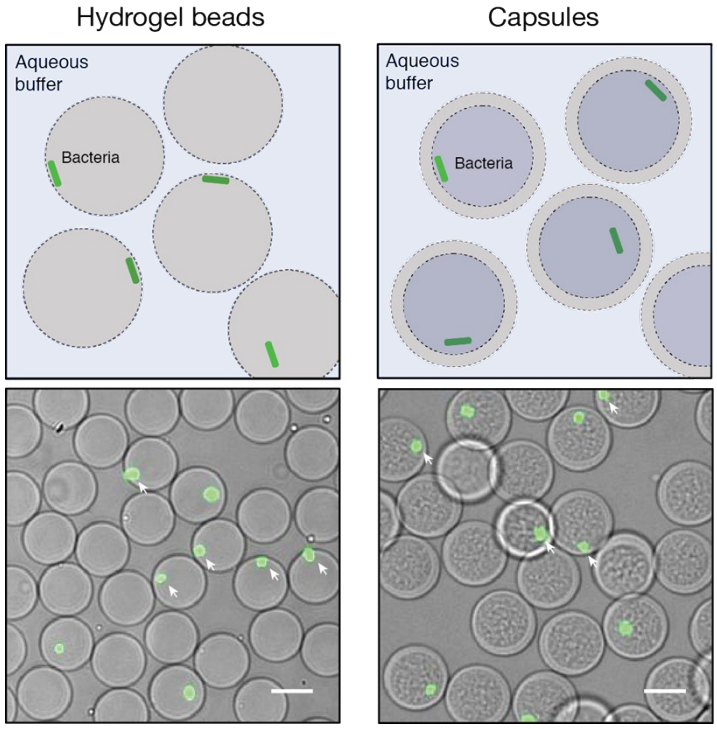

Supplementary Figure S6. **Bacteria distribution inside hydrogel beads and capsules.** *The left side shows the partition of encapsulated E. coli cells inside the hydrogel beads, and the right side shows the partition inside the capsules. The green fluorescent dots are bacteria stained with SYBR Green I dye. Note how encapsulated bacteria (white arrows) tend to partition at the PEGDA/water interface (left) or at the dextran/PEGDA interface (right). Scale bars, 20 µm.*

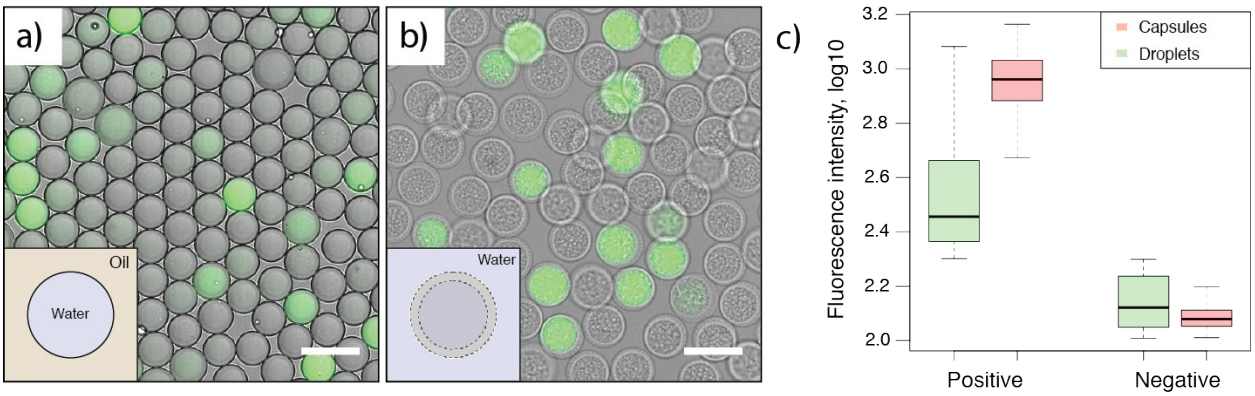

Supplementary Figure S7. SGA reaction yield on *B. subtilis* was more efficient in capsules than in water-in-oil emulsion. *Merged fluorescent and bright-field images of (a) post-SGA droplets and (b) post-SGA capsules. (c) Comparison of SGA reaction efficiency based on fluorescence intensity in droplets (green) and in capsules (red). "Positive" and "Negative" reactions correspond to compartments having encapsulated bacteria or having no bacteria, respectively. Boxplots are derived by measuring N>500 compartments for each reaction. Scale bars, 50 µm.*

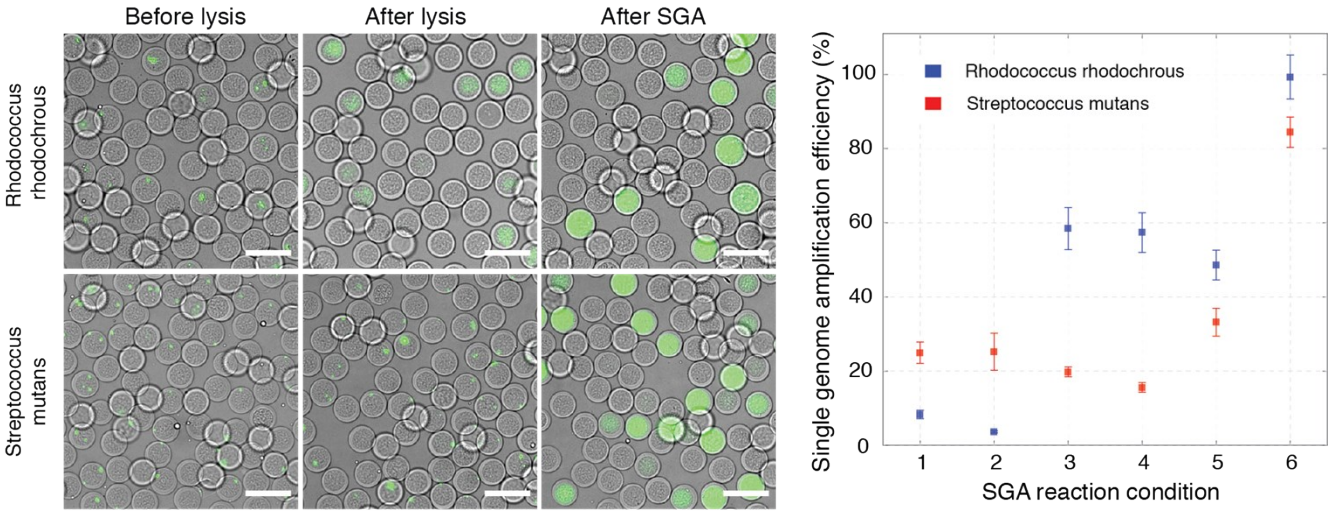

Supplementary Figure S8. Proteinase K and SDS treatment yielded the largest SGA on individual gram-positive cells using semi-permeable capsules. *On the left, digital images showing capsules stained with DNA binding dye (SYBR Green I) before lysis, after lysis, and after SGA. The following exposure times were used for fluorescent microscopy: before and after lysis – 1 s, after SGA – 10 ms. On the right, single genome amplification efficiency at different SGA reaction conditions using capsules (see Table 1 for details). Single genome amplification efficiency is expressed as a percentage of observed over expected DNA amplification reactions of gram-positive bacteria lysed and processed at different conditions. Scale bars, 50 µm.*

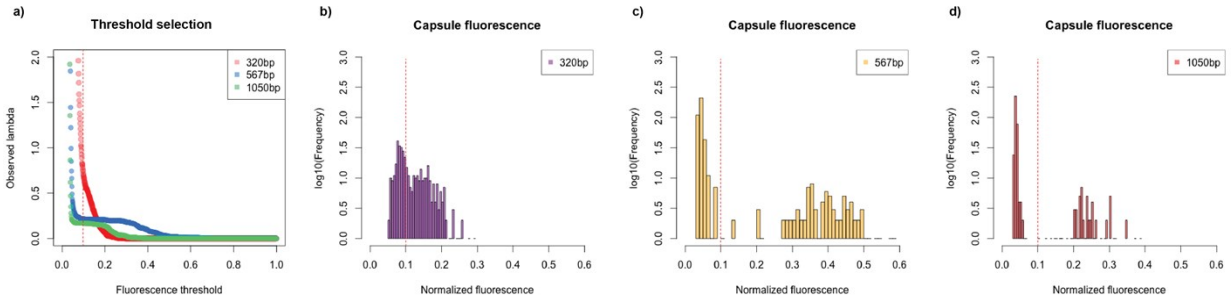

Supplementary Figure S9. PCR amplicon diffusion analysis in capsules. *a) Observed occupancy of capsules containing 320, 567 or 1050 bp. amplicon as a function of fluorescence threshold, b) normalized fluorescence intensity of capsules containing 320 bp PCR fragment, c) normalized fluorescence intensity of capsules containing 567 bp PCR fragment, and d) normalized fluorescence intensity of capsules containing 1050 bp PCR fragment. Dash line indicates the threshold value used to determine the occupancy values.*

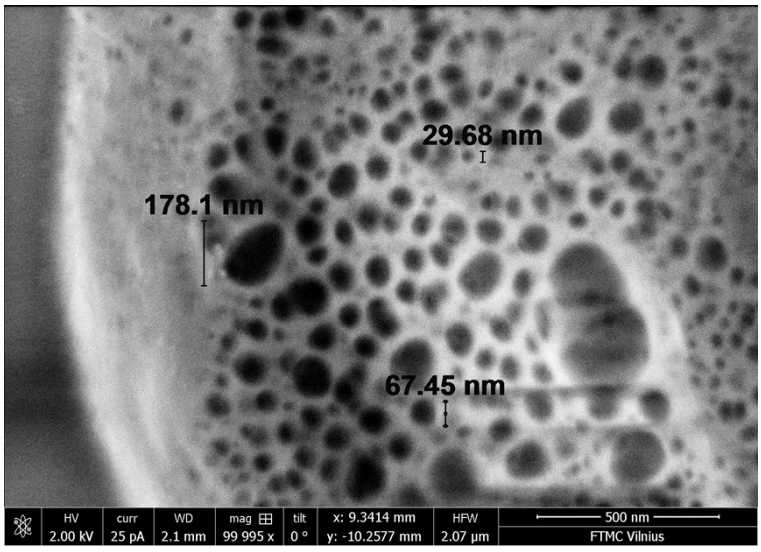

Supplementary Figure S10. Scanning electron microscopy reveal porous capsule structure. *The average pore size of a hydrogel shell measured with SEM is 55 ± 31 nm.*

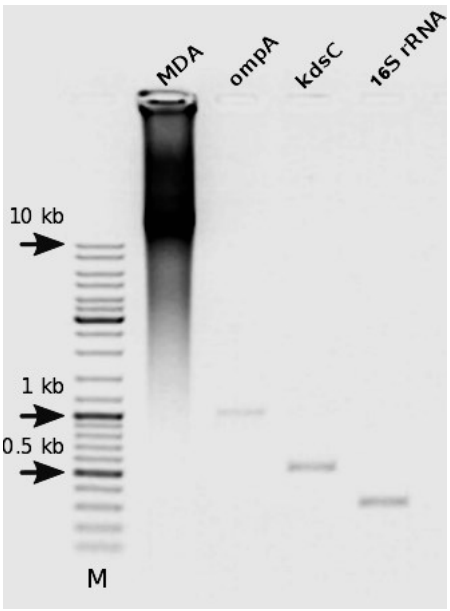

Supplementary Figure S11. **DNA recovery from post-PCR and post-SGA capsules by alkaline treatment.** *5 µl of capsules, harboring amplified DNA product were dissolved in 1M NaOH, neutralized with 1M acetic acid, and released DNA was purified/concentrated using AMPureXP magnetic beads. The expected size of ompA, kdsC and 16S RNA amplicons is 1050, 567 and 320 bp, respectively. M – GeneRuler DNA Ladder Mix (SM0331).*

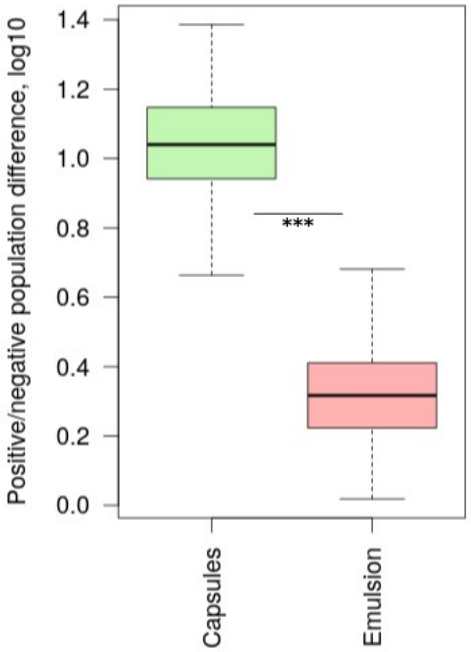

Supplementary Figure S12. **Signal-to-noise ratio is higher in capsules.** *Normalized fluorescence of droplets and capsules containing E. coli colonies after 4 hours growth. Boxplots are derived from samples of N>500 measurements, stars show statistical significance P<0.001 based on 2-tailed t-test.*

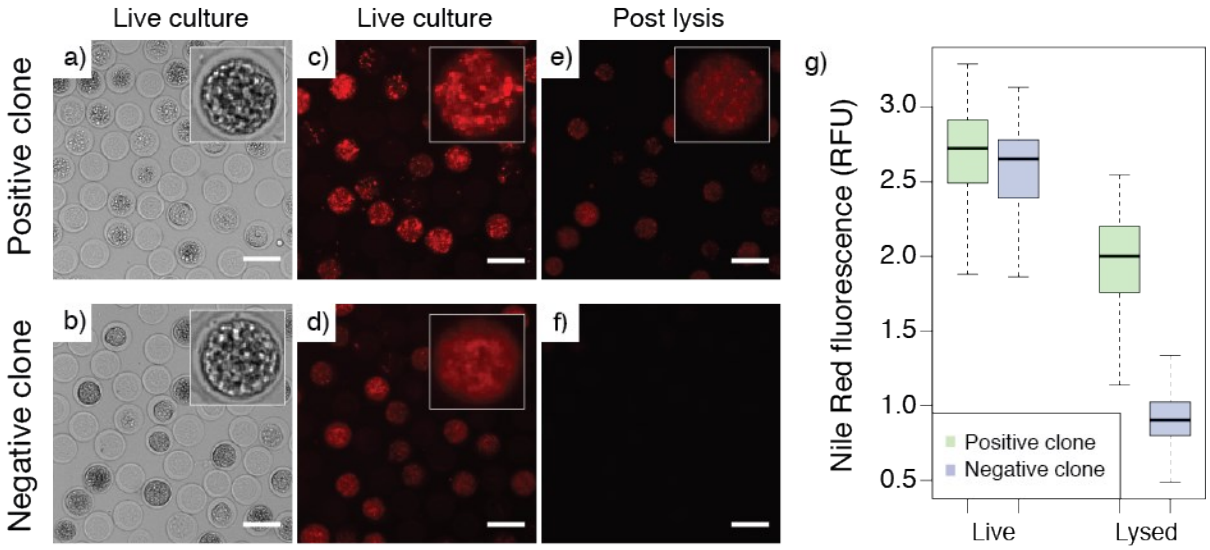

Supplementary Figure S13. **Phenotypic analysis of PHB-producing micro-colonies based on Nile Red staining.** *Live micro-colonies of bacteria producing PHB (a and c) and negative control (b and d) showing no significant difference in fluorescence due to staining of cellular membranes. Lysed micro-colonies of positive (e) and negative clones (f) after washing the capsules to remove solubilized membranes. (g) Boxplot showing relative PHB levels using Nile Red dye on live and lysed cells. Note how additional washing of capsules containing lysed cells increased the ability to resolve PHB expressing colonies from negative controls. Boxplots are derived by measuring N>100 compartments for each assay. Scale bars, 50 µm.*

Supplementary Note: Hydrogel pore size evaluation by PCR amplicon diffusion analysis

To test a diffusion of different length DNA amplicons we grew E. coli in a liquid LB media until O.D. ~ 0.5, diluted the bacterial suspension down to ~1.5 * 10^8 cells / mL and encapsulated for 60 min using a microfluidics device indicated in Figure 1. After capsule collection off-chip a small fraction (~1/10^{th}) was treated with SYBR Green I dye, which stained cellular DNA and enabled quantification of the initial occupancy value (λ) that was ≈ 0.2 (**Figure 3**, green boxplot). The unstained capsules were subjected to lysis conditions (50 U/µL lysozyme, 0.1% (v/v) Triton X-100, 1 mM EDTA, 200 µg/ml proteinase K, 10 mM Tris-HCl [pH 7.5] and after 30 min of incubation at 50 ºC a small fraction of capsules (~1/10^{th}) was stained again with SYBR Green I dye to quantify the post-lysis occupancy that, as expected, was close to initial $\lambda \sim 0.2$ (**Figure 3**, blue boxplot). Next, the capsules were evenly distributed into three 0.5 ml tubes and subjected to bulk PCR conditions (see Material and Methods) using a set of primers targeting one of the genes; 16S rRNA (320 bp amplicon), kdsC (567 bp amplicon) or ompA (1050 bp amplicon). After PCR, the capsules were stained with SYBR Green I dye and a number of fluorescent compartments was quantified under the microscope. One could expect that when there is no exchange of PCR amplicons between the capsules only those capsules that contained PCR product should be fluorescent and thus closely match the initial and post-lysis occupancy ($\lambda \sim 0.2$). Contrary, when there is a diffusion of PCR amplicons, the capsules containing PCR product should lose fluorescence and capsules that were empty should gain fluorescence leading to $\lambda > 0.2$. In our case we observed λ increase when PCR amplicon was 320 bp.. and no change ($\lambda \sim 0.2$) when PCR amplicons were ≥ 567 bp.

To illustrate the process of fluorescence threshold selection for measuring occupancy values, we present a graphical representation of how λ changes with threshold variation (**Supplementary Figure S9a**). It can be seen that for 1050 and 567 bp fragments there is a relatively flat region around *x = 0.15* (15% of max pixel intensity), where lambda value does not significantly depend on the fluorescence threshold. Due to the diffusivity of shorter fragments and greater variation of fluorescence among resulting capsules, there is no such region for 320 bp fragments, only a small inflection point, at *x = 0.1*, which can be used to classify positive and negative capsules. We therefore set a fluorescence threshold at 0.1 to estimate the occupancy of each sample.

Alternatively, by plotting the histogram for each PCR condition **Supplementary Figure S9b-d** we observe a clear separation between negative (empty) and positive (containing PCR amplicon) capsules with either 1050 or 567 bp. fragment. There is no clear separation of negatives/positives when capsules contain 320 bp. fragment indicating the PCR fragment diffusion and exchange between the capsules. One can estimate the approximate radii of gyration of DNA fragments and approximate the observed diffusivity to the hydrogel pore size through the Kratky-Porod equation:

$$\left\langle R_G^2(M)\right\rangle \approx \frac{b_K L_D}{6}\left[1-3\left(\frac{b_K}{2L_D}\right)+6\left(\frac{b_K}{2L_D}\right)^2-6\left(\frac{b_K}{2L_D}\right)^3\left(1-e^{-2L/b_K}\right)\right],$$

where b_K is the polymer Kuhn length, R_g is radius of gyration, L_D is the total contour length expressed as $L_D = Mb$, here M is the molecular weight (number of monomers) and b is monomer size. For dsDNA, the Kuhn length is typically $b_K \approx 100$ nm and $b \approx 0.34$ nm.

Using the above expression, we estimate the PCR amplicons of 320, 567 and 1050 bp. size to have radii of gyration on the order of 26, 40 and 60 nm, respectively. Considering these values and diffusivity results, it can be approximated that the average pore size of the hydrogel shell is approximately ~30 nm.